

Contact and non-contact photothermal calorimetry for investigation of condensed matter

Trends and recent developments

D. Dadarlat

CEEC-TAC1 Conference Special Issue
© Akadémiai Kiadó, Budapest, Hungary 2012

Abstract This article is a review of new possibilities offered by two photothermal (PT) methods, a contact (photopyroelectric (PPE) calorimetry) and a non-contact one (photothermal radiometry (PTR)) for accurate measurements of dynamic thermal parameters (thermal diffusivity and effusivity) of condensed matter samples. Among a large variety of detection configurations, we selected in the article a recent proposed one, allowing for coupled PPE–PTR experiments. The detection cell of such a configuration is composed by a directly irradiated pyroelectric sensor, a liquid layer (coupling fluid) and a solid/liquid backing material. The measurements are based on the thickness scanning procedure of the coupling fluid (TWRC technique). Some recent applications concerning measurements of thermal diffusivity and effusivity of some liquids and solids (thin layers or bulk materials) together with a study of the accuracy of the investigations are described.

Keywords PPE calorimetry · PTR calorimetry · Thermal parameters · TWRC method · Condensed matter

Introduction

During the last decades the photothermal (PT) techniques, overtook the stages of development of theoretical aspects and qualitative applications. People working in the field are now exploring the limits of the methods for accurate investigations of thermal properties of condensed matter. In

principle, in all PT techniques a heat is generated in a sample due to the absorption of an incident radiation. The heat developed in the material can produce several effects as: temperature and refractive index gradients, geometrical displacements, acoustic waves, changes in the emitted IR spectrum, etc. Each of these effects is associated with at least one PT technique. We can count as main PT methods: (i) the photopyroelectric (PPE) technique (based on the direct measurement of thermal gradients); (ii) the thermal lensing (TL) and photothermal beam deflection (PBD) (based on the use of refractive index gradients); (iii) the photoacoustic (PA) technique (based on the effects of the acoustic waves produced by the heat propagation); and the photothermal radiometry (PTR) (based on the change of the IR spectrum of the heated sample); etc. [1–3]. All these methods have as final purposes the measurement of the quantity of heat generated in the sample, and the study of its propagation through the material. In such a way, one can obtain the values of all sample's related static (specific heat) and dynamic (thermal diffusivity, effusivity and conductivity) thermal parameters and to study physical processes associated with the change of these thermal parameters as a function of temperature, time, composition, etc. [1–3].

The information, obtained in a PT experiment can be collected directly (by measuring with a “thermometer” the temperature gradients) or indirectly, following several steps (e.g. the thermal gradients produce gradients of refractive index—as a consequence a probe laser beam, is deflected and this deflection is measured with a position sensor, etc.) [4].

The first methods are called contact techniques, because the sensor is in direct contact with the sample; the best example is the PPE technique, in which a sample is irradiated with a modulated optical radiation and the temperature increase of the sample is measured with a pyroelectric sensor in thermal contact with the material. The techniques

D. Dadarlat (✉)
National R&D Institute for Isotopic and Molecular
Technologies, Donath Str. 65-103, POB-700,
400293 Cluj-Napoca, Romania
e-mail: ddadarlat@gmail.com

that follow several steps to measure the heat developed in the sample are noncontact techniques, because the final transducer (IR detector for PTR, position sensor for PBD, photodiode for TL, microphone for PA) are not in contact with the investigated material. In the PTR method, for example, the increase of the temperature at the surface of the irradiated sample produces a modified IR emitted spectrum; the IR radiation is collected with an IR detector, and the processed signal from the sensor contains information about the sample’s thermal parameters [1–5].

In this article, we will review the main features of two PT calorimetries, a contact, PPE, and a non-contact one, PTR. As “recent developments and trends” concerning these methods, we will focus on two recent improvements: (i) the increase of the number of the layers of the PPE detection cell (with the final purpose of measuring the thermal parameters of a thin solid and/or all thermal parameters of a liquid in a self-consistent manner) and (ii) the possibility of combining the two methods in one experiment.

The main theoretical aspects of the two techniques and a new designed experimental setup for a combined PPE–PTR detection cell will be described. Some calorimetric applications on condensed matter samples (various liquids and thin/thick solids) will point out the performances of this combined technique.

Theory

The layout of the detection configuration of a combined PPE–PTR detection cell is shown in Fig. 1. The detection cell usually contains 3 layers (pyroelectric sensor/liquid layer (coupling fluid)/semi-infinite solid backing). When the backing is liquid, an additional thin solid layer must be inserted between the backing and the coupling fluid to separate the two liquids (4-layers cell). The radiation is partially absorbed by the front, opaque electrode of the thermally thin pyroelectric sensor. Air and backing layers are considered semi-infinite. In order to obtain the PPE and PTR signals, one has to solve the classical thermal

diffusion equations with the boundary conditions for temperature and flux continuity and finally, to deduce the temperature at the front surface of the sensor (PTR), and to integrate the temperature distribution over the sensor’s thickness (PPE). We will present in this review only some steps of the calculations. Analytical details can be found in Refs. [6] and [7].

PPE

For a 4-layers cell, the temperature across the directly irradiated pyroelectric sensor is given by [7–9]:

$$\Theta(x) = \frac{H_0}{4k_1\sigma_1} \frac{(1 + R_{01}) [e^{-\sigma_1 x} + \rho_{21} e^{-\sigma_1(2L_1-x)}]}{1 - R_{01}\rho_{21} e^{-2\sigma_1 L_1}} \tag{1}$$

where H_0 represents the incident flux and

$$R_{01} = \frac{1 - b_{01}}{1 + b_{01}} = 1; \rho_{21} = \frac{(1 - b_{21}) + \rho_{32}(1 + b_{21})e^{-2\sigma_2 L_2}}{(1 + b_{21}) + \rho_{32}(1 - b_{21})e^{-2\sigma_2 L_2}}$$

$$\rho_{32} = \frac{(1 - b_{32}) + \rho_{43}(1 + b_{32})e^{-2\sigma_3 L_3}}{(1 + b_{32}) + \rho_{43}(1 - b_{32})e^{-2\sigma_3 L_3}}; \rho_{43} = \frac{1 - b_{43}}{1 + b_{43}} \tag{2}$$

In order to obtain the photopyroelectric signal, we have to integrate Eq. 1 over the thickness of the pyroelectric sensor.

$$V^{PPE} = \int_0^{-L_1} \Theta(x) dx. \tag{3}$$

If we normalize the signal obtained with a 4-layers cell to the signal obtained with semi-infinite coupling fluid, we obtain for the normalized complex PPE signal:

$$V_n^{PPE} = \frac{1 - R_{21} e^{-2\sigma_1 L_1}}{1 - \rho_{21} e^{-2\sigma_1 L_1}} \times \frac{(e^{-\sigma_1 L_1} - 1) - \rho_{21}(e^{-\sigma_1 L_1} - e^{-2\sigma_1 L_1})}{(e^{-\sigma_1 L_1} - 1) - R_{21}(e^{-\sigma_1 L_1} - e^{-2\sigma_1 L_1})} \tag{4}$$

with

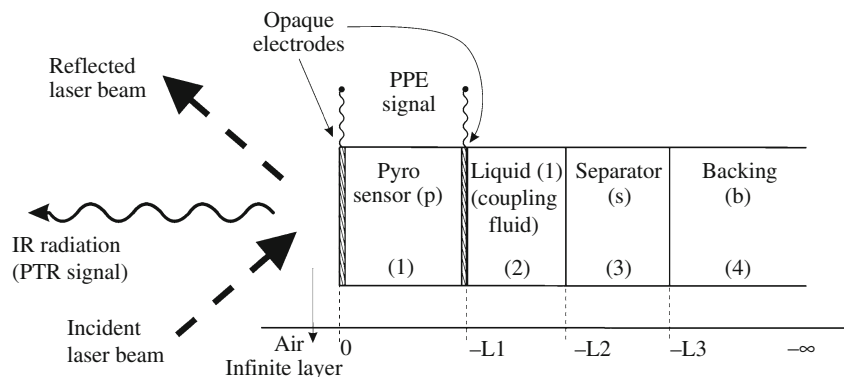


Fig. 1 Layout of the 4-layers detection cell. For a 3-layers detection cell the backing material is a solid and the separator layer is missing

$$R_{21} = \frac{1 - b_{21}}{1 + b_{21}} \quad (5)$$

In Eqs. 1–5 $\sigma_j = (1 + i)a_j$, $\mu = (2\alpha/\omega)^{1/2}$, $b_{ij} = e_i/e_j$, α and e are the thermal diffusivity and effusivity, ω is the angular chopping frequency of radiation, σ and a are the complex thermal diffusion coefficient and the reciprocal of the thermal diffusion length ($a = 1/\mu$), respectively.

For a 3-layers detection cell (layer 3 in Fig. 1 is missing), Eq. 4 reduces to [10, 11]:

$$V_n^{\text{PPE}} = \frac{\sigma_1 L_1 + b_{21}}{(\sigma_1 L_1) + b_{21} \left(\frac{1 - R_{42} \exp(-2\sigma_2 L_2)}{1 + R_{42} \exp(-2\sigma_2 L_2)} \right)}. \quad (6)$$

PTR

If the irradiated sensor is optically opaque, the thermal radiation emittance of a material is given by $\delta W = 4\varepsilon\sigma_B T_0^3 \delta T$, where ε is the sample's emissivity, σ_B is the Stephan–Boltzmann constant, T_0 is the steady state temperature, and T the sample's surface temperature [7, 12].

From experimental point of view, PTR is generally used only with a 3-layers cell (the influence of a 4-th layer on the sensor's surface temperature variation is low). Using the classical procedure, for a 3-layers cell (separator missing), the fluctuations of the sample's surface temperature are given by [9]

$$\delta T = \frac{Q_0}{2k_1 \sigma_1} \frac{1 + R_{21} \exp(-2\sigma_1 L_1)}{1 - R_{21} \exp(-2\sigma_1 L_1)} \quad (7)$$

where Q_0 is the absorbed radiant flux.

$$R_{21} = \frac{1 - b_{21} + R_{42}(1 + b_{21}) \exp(-2\sigma_2 L_2)}{1 + b_{21} + R_{42}(1 - b_{21}) \exp(-2\sigma_2 L_2)}; \quad (8)$$

Combining Eqs. 7 and 8, we obtain for the PTR signal:

$$V_n^{\text{PTR}} = \frac{4K(f)\sigma_B T_0^3 \varepsilon Q_0}{2k_1 \sigma_1} \frac{1 + R_{21} \exp(-2\sigma_1 L_1)}{1 - R_{21} \exp(-2\sigma_1 L_1)} \quad (9)$$

where $K(f)$ is an instrumental factor depending on the geometry of the system and electronic transfer function.

After normalization with semi-infinite coupling fluid layer, we get:

$$V_n^{\text{PTR}} = \frac{A_- B_+}{A_+ B_-} \quad (10)$$

where

$$\begin{aligned} A_{\pm} &= 1 + b_{21} \pm (1 - b_{21}) \exp(-2\sigma_1 L_1) \\ B_{\pm} &= \left\{ 1 + b_{21} + R_{42}(1 - b_{21}) \exp(-2\sigma_2 L_2) \right. \\ &\quad \left. \pm [1 - b_{21} + R_{42}(1 + b_{21}) \exp(-2\sigma_2 L_2)] \exp(-2\sigma_1 L_1) \right\} \end{aligned} \quad (11)$$

We can conclude that both normalized PPE and PTR signals (Eqs. 4–6, 10 and 11) depend on the thermal

diffusivity and effusivity of the pyroelectric sensor, liquid layer (coupling fluid) and separator (for the 4-layers cell) and on the thermal effusivity of the backing material. Performing a thickness scan of the amplitude and/or phase of the PPE and PTR signals, at constant chopping frequency (TWRC method) [7, 8, 13–16], one can get information about one, or eventually two layers of the detection cell.

Mathematical simulations for the phase of the PPE and PTR signals (phase is mostly used in experiments than the amplitude) are displayed in Fig. 2 [7]. The simulations were performed considering a 150 μm thick LiTaO₃ pyroelectric sensor ($e_p = 3.92 \times 10^3 \text{ W s}^{1/2} \text{ m}^{-2} \text{ K}^{-1}$; $\alpha_p = 1.56 \times 10^{-6} \text{ m}^2 \text{ s}^{-1}$), water ($e_l = 1.6 \times 10^3 \text{ W s}^{1/2} \text{ m}^{-2} \text{ K}^{-1}$; $\alpha_l = 14.6 \times 10^{-8} \text{ m}^2 \text{ s}^{-1}$) as liquid layer and 1 Hz chopping frequency; (“p” pyroelectric sensor; “l” liquid layer (coupling fluid); “b” backing layer). Four materials, with thermal effusivity ranging from 400 $\text{W s}^{1/2} \text{ m}^{-2} \text{ K}^{-1}$ (low thermal conductors) to 35,000 $\text{W s}^{1/2} \text{ m}^{-2} \text{ K}^{-1}$ (good thermal conductors), were inserted as backing.

The theory developed in this section, together with the simulations from Fig. 2, indicates that, in all cases, for both PPE and PTR signals, the information can be extracted only from the thermally thin regime for the sensor and liquid layer. In the thermally thick regime for the sensor and/or liquid layer, both amplitude and phase saturate. The sensitivity of the methods depends on the effusivity ratio of the backing/liquid layer. The very similar behaviours of the PPE and PTR signals give the opportunity to obtain information in *the same thickness range*; in conclusion, in one experimental run (one thickness scan), we can extract both PPE and PTR information. The thermally thick regime

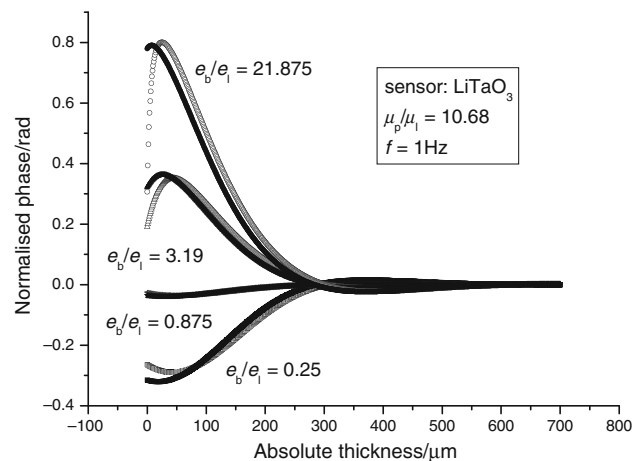
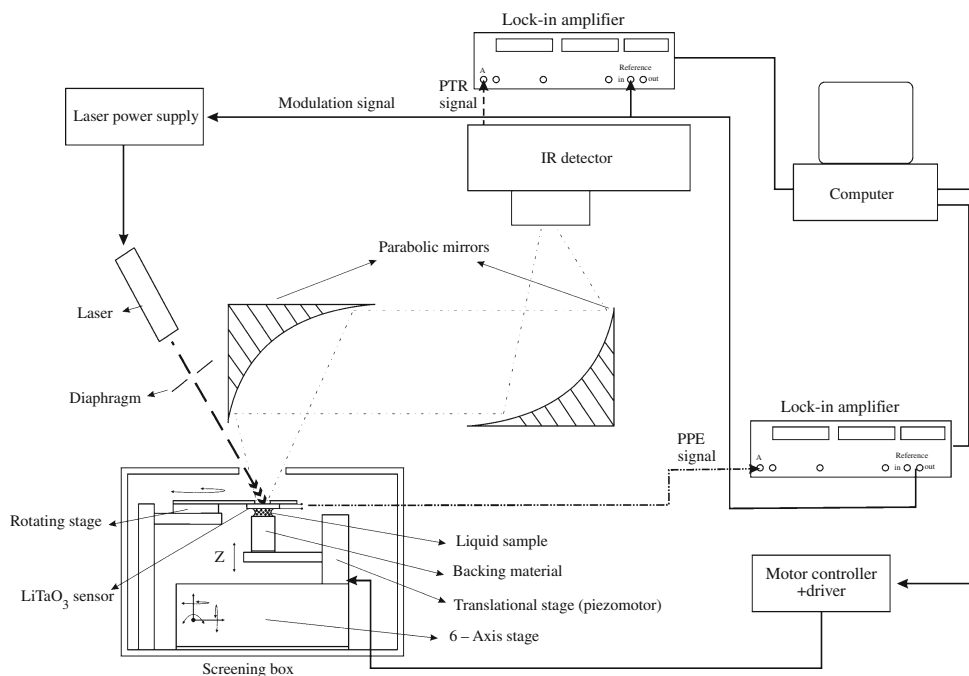


Fig. 2 Mathematical simulations of the behaviour of the normalized phase of the FPPE (*empty symbols*) and PTR (*filled symbols*) signals as a function of coupling fluid's thickness (water) for different backing/coupling fluid effusivity ratios (pyroelectric sensor-150 μm thick, chopping frequency-1 Hz, $\mu_p/\mu_l = 10.68$). “p” pyroelectric sensor; “l” liquid layer (coupling fluid); “b” backing layer

Fig. 3 Combined PPE–PTR–TWRC experimental set-up



for the coupling fluid, combined with the thermally thin regime for the sensor (the region 500–700 μm from Figs. 2 and 3) is used for normalization purposes. Consequently, the normalization signal is contained in the same scanning run (no additional measurement is necessary). We have also to stress on the fact that the two methods preserve all the advantages of the TWRC technique [13–17]. The most important (if compared with frequency scanning procedures) is the possibility of keeping a thermally thin regime for the sensor, thermally thick for the backing and changing the thermal regime of the liquid from thermally thin to thermally thick.

Experiment

The design of the experimental set-up is shown in Fig. 3 [18]. The pyroelectric sensor, a 100–300 μm thick LiTaO_3 single crystal ($\epsilon_p = 3.66 \times 10^3 \text{ W s}^{1/2} \text{ m}^{-2} \text{ K}^{-1}$; $\alpha_p = 1.36 \times 10^{-6} \text{ m}^2 \text{ s}^{-1}$), provided with Cr–Au electrodes on both faces, is glued on a rotating stage. The backing material is situated on a micrometric stage. The modulated radiation (30 mW YAG laser) is partially absorbed by the front electrode of the sensor. The space between the sensor and the backing material accommodates the liquid layer. The liquid's thickness variation is performed with a step of 0.03 μm (9062 M-XYZ-PPP Gothic-Arch-Bearing Pico-motor) and the data acquisition was taken each 30-th step. The “rough” control of the liquid's thickness and the parallelism between backing and sensor are assured by 3- and 6-axis micrometric stages. During the scanning procedure, the sample's thickness variation is very rigorously

controlled, but the absolute sample's thickness it is not precisely known. Its correct value is obtained as a result of a fitting procedure [13, 14]. The IR radiation emitted by the pyroelectric sensor was collected with parabolic mirrors and sent on the surface of a cooled HgCdTe IR detector.

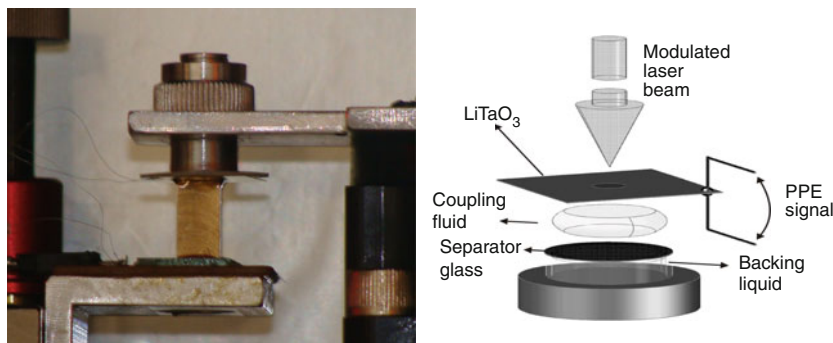
All the measurements were performed at room temperature. The PPE and PTR signals were processed with SR 830 lock-in amplifiers. The internal oscillator of the lock-in, used in PPE measurements, gave the reference signal for the second lock-in and assured, in the same time, the modulation of the incident radiation. The data acquisition, processing and analysis were performed with adequate software. Details for the sensor-sample assembly are displayed in Fig. 4.

Recent applications

During last decades a lot of applications were reported, both for PPE and PTR calorimetry and they concerned highly accurate investigations of thermal parameters of solids and liquids [6, 10, 11, 13, 16–22]. Using for example the PPE calorimetry in various configurations, the thermal diffusivity [11, 13, 16, 17] and effusivity [11, 17, 19, 22] of the coupling fluid, and the thermal effusivity of a bulk backing solid [6, 10, 19] were obtained with high accuracy, for a 3-layers detection cell. The PTR calorimetry was intensively used to measure thermal diffusivity and effusivity of solids inserted as first layer in a 2-layers detection cell [18, 21].

As mentioned in the “Introduction” section, in this review we will focus only on some recent results: they

Fig. 4 Details of the sensor-sample assembly. *Left* photo of the cell with solid backing material. *Right* schematic of the detection cell for liquid materials inserted as backing layer



were obtained with PPE calorimetry when extended the number of layers of the detection cell from 3 to 4 and with combined PPE–PTR calorimetry for a 3-layers detection cell. In all cases the scanning parameter is the thickness of the coupling fluid (TWRC method) [13–16].

4-Layers PPE detection cell

A 4-layers PPE detection cell is necessary when the backing layer is a liquid [23]. In such a case, a thin solid separator layer must be inserted between the coupling fluid and the backing liquid. A 4-layers cell presents two clear advantages compared with the 3-layers one: (i) it offers the possibility of measuring the thermal parameters of the thin solid layer inserted as separator and (ii) it allows the direct measurement of thermal diffusivity and effusivity of a liquid, by a self-consistent procedure. These two applications will be described in the following.

PPE calorimetry of thin solids [24]

If we refer to thin solid layers, they are nowadays widely used in many fields, and consequently, their physical (optical, electrical and thermal) properties are of great interest. Concerning the thermal properties of thin layers, they can be completely different from the properties of bulk materials. The main reason is that the heat transport in solids is very sensitive to the intimate structure and often thin layers contain defects that restrict heat transport by phonons. If the thin solid layer is deposited on a substrate, the interfacial layer between the film and the substrate forms a thermal barrier and lowers the effective thermal conductivity of the film. This is why the measurement of thermal parameters (especially the dynamic ones: thermal diffusivity, conductivity and effusivity) of thin layers is a complicated problem; noncontact methods on thin layers that are not deposited on substrates are preferable.

In this section, we present results of the PPE calorimetry for measuring the thermal diffusivity, or effusivity of a thin solid layer. We have to mention that one thermal parameter

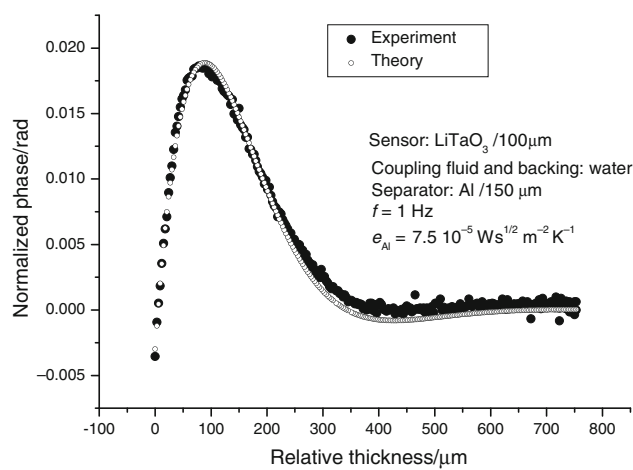


Fig. 5 The experimental behaviour of the normalized PPE phase as a function of coupling fluid's thickness, for a detection cell with 150 μm thick Al foil as separator. The best theoretical fit is also displayed

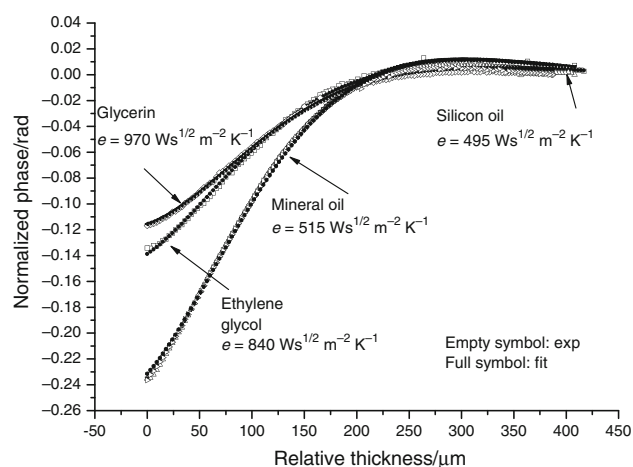


Fig. 6 Normalized phase of the complex PPE signal as a function of the thickness of coupling fluid, for a cell containing water as coupling fluid and different liquids (glycerine, ethylene glycol, mineral and silicon oils) as backing liquids. Full points represent the best fit performed with Eq. 4

can be obtained, only if the other one is known (in the following we consider thermal diffusivity as an unknown parameter). The detection cell is that from Fig. 1, but liquids (2) and (4) are identical.

A typical plot of the behaviour of the normalized phase of the PPE signal as a function of relative thickness of the coupling fluid, for a good thermal conductor (separator—150 μm thick Al) is displayed in Fig. 5. The chopping frequency of radiation was 1 Hz and the two liquids (2) and (4) are water. Fig. 5 contain also the best fit performed with Eq. 4 on the experimental data. The results obtained on other thin solid layers are in good agreement with previously reported data [25].

Self-consistent PPE calorimetry of liquids [26]

In this section, the PPE technique in front configuration, together with the thermal-wave resonator cavity (TWRC) method is applied to measure both thermal effusivity and diffusivity of liquids. The methodology is based on a 4-layers detection cell (Fig. 1) in which the investigated liquid is inserted successively in backing and in coupling fluid’s position, respectively. When inserted in the backing position a scan of the phase of the PPE signal as a function of (a known) coupling fluid’s thickness leads to the direct measurement of liquid’s thermal effusivity. Inserting then the investigated liquid in coupling fluid’s position (with a known backing liquid), a similar thickness scan leads to the measurement of its thermal diffusivity. In such a way, the PPE–TWRC method becomes self-consistent; all static and dynamic thermal parameters can be derived with the same technique (two of them are directly measured and the remaining two calculated). The suitability of the method is demonstrated in the following with investigations on several liquids as water, ethylene glycol, glycerine and various oils.

Typical results for the normalized phase of the PPE signal for a detection cell containing water as coupling fluid and various liquids in the backing position are presented in Fig. 6, together with the best fits performed with Eq. 4. The fit was performed with two fitting parameters: coupling fluid’s absolute thickness and backing’s thermal effusivity.

Figure 7 displays a similar graph, but in this case, water was the liquid in the backing position, and the investigated liquids played the role of coupling fluid. As presented in the “Theory” section, in such a case the phase of the signal depends on both thermal effusivity and diffusivity of the coupling fluid; having the value of the thermal effusivity from the previous measurement, one can obtain the value of coupling fluid’s thermal diffusivity by performing a fit with coupling fluid’s absolute thickness and its thermal diffusivity as fitting parameters.

Table 1 Thermal parameters of the investigated liquids, together with literature data

Liquid	Thermal parameters				Lit.	Thermal parameters			
	$e/W \text{ s}^{1/2} \text{ m}^{-2} \text{ K}^{-1}$	$\alpha \times 10^8 / \text{m}^2 \text{ s}^{-1}$	$C \times 10^{-4} / \text{J m}^{-3} \text{ K}^{-1}$ (calc.)	$k/W \text{ m}^{-1} \text{ K}^{-1}$ (calc.)		$e/W \text{ s}^{1/2} \text{ m}^{-2} \text{ K}^{-1}$	$\alpha \times 10^8 / \text{m}^2 \text{ s}^{-1}$	$C \times 10^{-4} / \text{J m}^{-3} \text{ K}^{-1}$ (calc.)	$k/W \text{ m}^{-1} \text{ K}^{-1}$
Ethylene glycol	840 ± 38	9.60 ± 0.45	271 ± 6	0.26 ± 0.02	[27, 28]	814	9.38	266	0.2569; 0.249
Silicon oil	495 ± 37	7.40 ± 0.55	182 ± 7	0.14 ± 0.02	[27]	506	7.01	191	0.1439; 0.134
Glycerine	970 ± 37	8.40 ± 0.33	335 ± 6	0.28 ± 0.03	[29, 30]	920; 933	9.38; 9.9	301; 297	0.28; 0.29
Mineral oil	515 ± 38	6.20 ± 0.47	207 ± 8	0.13 ± 0.01	[26, 27]	592	5.25; 5.60	258; 250	0.1307; 0.14

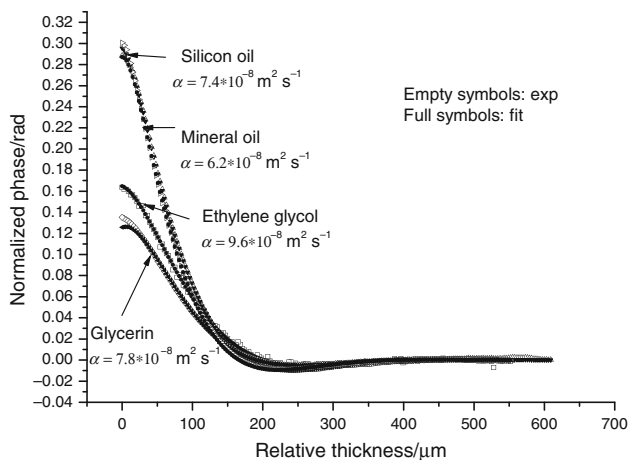


Fig. 7 Normalized phase of the complex PPE signal as a function of the thickness of coupling fluid, for a cell containing the investigated liquids (glycerine, ethylene glycol, mineral and silicon oils) as coupling fluids and water as backing liquid. Full points represent the best fit performed with Eq. 4

Table 2 Room temperature values of thermal effusivity for the investigated solids, as obtained from PPE and PTR measurements, together literature data

Material	Thermal effusivity/ $W s^{1/2} m^{-2} K^{-1}$		
	PPE	PTR	Literature
Steel	6,400	4,900	6,090–7,187 [3, 31]
Glass	1,360	1,280	1,275–1,600 [3–32]
Textolite	1,040	1,020	1,000–1,810 [3]
Dental polymer	980	980	870–1,110 [6]
Bakelite	760	680	681 [3]
Teflon	690	690	600–700 [3]
Propylene	520	490	–

Table 1 presents the results for all thermal parameters of the investigated liquids, obtained with the self-consistent PPE–TWRC method, together with literature data. The values of the thermal conductivity and volume specific heat were calculated, using well known formulas: $k = \alpha C$, $\alpha = (Ck)^{1/2}$. The obtained results are in good agreement with literature data.

Combined PPE–PTR calorimetry of bulk solids

In this section, the PPE and PTR calorimetries are simultaneously used, together with the thermal-wave resonator cavity method, to investigate the thermal effusivity of solids inserted as backing layers (3-layers detection cell). The main result is the possibility offered by the PTR technique, to provide calorimetric information about the third layer of a detection cell.

Typical thickness scans of the phase of the PPE and PTR signals for a detection cell containing ethylene glycol as

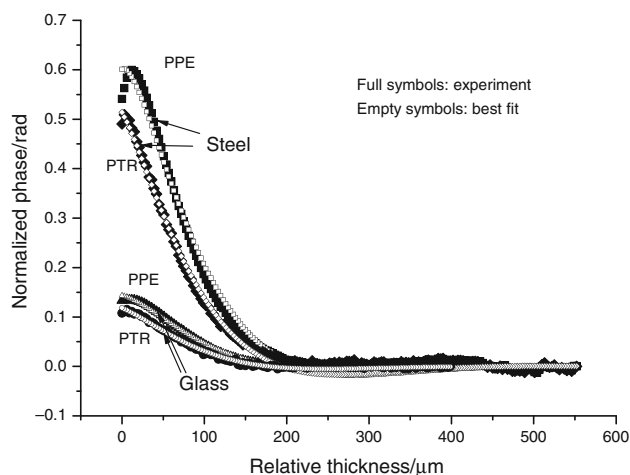


Fig. 8 The behaviour of the phase of the PPE and PTR signals for a cell containing ethylene glycol as coupling fluid and two backing materials with different values of thermal effusivity

coupling fluid and two types of solid backing materials with different values of thermal effusivity (steel and glass) are displayed in Fig. 8, together with the best fit performed with Eqs. 6, 10 and 11, respectively.

Table 2 indicates that the results obtained for the thermal effusivity of the investigated solids, with the two techniques, PPE and PTR (a contact and a non-contact one), are in good agreement and they also agree with literature data. In fact, the agreement is better for low thermal conductors. The discrepancies observed for good thermal conductors can be explained by tacking into account the accuracy of the measurements [23].

Discussions and conclusions

This review describes some recent possibilities offered by two PT methods, a contact (PPE) and a non-contact one (PTR) for accurate measurements of dynamic thermal parameters (thermal diffusivity and effusivity) of condensed matter samples. Among a large variety of detection configurations we selected a recent proposed one, allowing for simultaneous PPE–PTR experiments; both methods are based on TWRC technique.

As presented in the “Theory” section a combined PPE–PTR detection cell, can contain 3 or 4 layers. For the proposed configuration the second layer is always a liquid, whose thickness is scanned (TWRC method). It is important to note that the information is contained both in the amplitude and phase of the PPE and PTR signals and it can concern any layer of the detection cell. Practically, with such a method, one can directly measure the thermal diffusivity and effusivity of the first 2 (or 3) layers and the thermal effusivity of the last (3-rd or 4-th) one. The values

of the unknown thermal parameters were always obtained through fitting procedures and generally, the phase of the signals was used as source of information, due to a better signal/noise ratio.

Concerning the experimental set-up, its main particularity is the detection cell. It contains as first, irradiated layer, the pyroelectric sensor, situated in a fixed position. The backing layer is supported by a translational stage, responsible for the thickness scan of the liquid layer (coupling fluid) accommodating the space between sensor and backing. When the backing is a liquid, some special cells must be designed to accommodate the liquid and to prevent its leakage and evaporation.

The applications described in this review were split in two.

The first set of applications was focused on the additional information possible to be obtained when working with a 4-layers PPE detection cell. The increase of the number of layers of a PPE detection cell from 3 to 4 was firstly imposed by the necessity of investigating volatile liquids [33]. Such liquids could not be inserted in a coupling fluid position due to their volatility, so they had to be inserted in backing position and consequently, special cells were designed (see Fig. 4). In this article, we suggested two new possible applications of the 4-layers PPE detection cell. One refers to the possibility of measuring the thermal parameters of thin solids (not deposited on substrates), and the second one to the complete characterization (self-consistent measurement of all 4 thermal parameters) of a liquid, by a proper alternation of the investigated liquid and a known liquid in two (backing and coupling fluid) positions [26].

The second set of applications takes into account the possibility of coupling the two PPE and PTR techniques, together with TWRC scanning procedure, for thermal characterization of condensed matter samples. In this article, the coupled PPE–PTR–TWRC method was used for measuring the thermal effusivity of bulk solids inserted as backing layers in the detection cell, but in fact, the technique can be used for thermal characterization of any layer of the detection cell.

Looking to the accuracy of the PPE–PTR–TWRC method, the PPE and PTR results are in good agreement and agree also with literature data. However, there is a discrepancy the between the results obtained with PTR and PPE and, as a general trend, it increases with increasing value of thermal effusivity of the backing. From both theory and experiment, it came out that the accuracy of both methods is higher when the values of thermal effusivity of backing layer and coupling fluid are close.

As a final remark, the two methods, as presented in this article, will always support each other, but they are not able, at this stage, to give complementary information,

because Eqs. 4, 10 and 11, respectively, contain the same thermal parameters.

Acknowledgements This study was supported in part by the Romanian Ministry of Education and Research Youth and Sport, through the National Research Program, PN-II-ID-PCE-2011-3-0036.

References

- Hess P, Pelzl J, editors. Photoacoustic and photothermal phenomena, Springer Ser. Opt. Sci. Vol. 58. Berlin Heidelberg: Springer; 1988.
- Murphy J, Maclachlan-Spicer JW, Aamodt LC, Royce BSH, editors. Photoacoustic and photothermal phenomena II, Springer Ser. Opt. Sci. Vol. 58. Berlin Heidelberg: Springer; 1988.
- Mandelis A. Principles and perspectives of photothermal and photoacoustic phenomena. New York: Elsevier; 1992.
- Tam AC. Applications of photoacoustic sensing techniques. *Rev Mod Phys.* 1986;58:381–431.
- Bicanic D, editor. Photoacoustic and photothermal phenomena III, Springer Ser. Opt. Sci. Vol. 58. Berlin Heidelberg: Springer; 1991.
- Dadarlat D, Streza M, Pop MN, Tosa V, Delenclos S, Longuemart S, Sahraoui AH. Photopyroelectric calorimetry of solids. FPPE–TWRC method. *J Therm Anal Calorim.* 2010;101:397–402.
- Dadarlat D, Pop MN, Streza M, Longuemart S, Depriester M, Sahraoui AH, Simon V. Combined FPPE–PTR calorimetry involving TWRC technique. Theory and mathematical simulations. *Int J Thermophys.* 2010;31:2275–83.
- Mandelis A, Matvienko A. Photopyroelectric thermal-wave cavity devices-10 years later. In: Denis Remiens, editor. Pyroelectric materials and sensors. Trivandrum: Research Signpost; 2007. p. 61–96.
- Mandelis A. Diffusion-Wave Fields: Mathematical Methods and Green Functions. New York: Springer; 2006.
- Streza M, Pop MN, Kovacs K, Simon V, Longuemart S, Dadarlat D. Thermal effusivity investigations of solid materials by using the thermal-wave-resonator-cavity (TWRC) configuration. Theory and mathematical simulations. *Laser Phys.* 2000;19:1340–4.
- Dadarlat D. Photopyroelectric calorimetry of liquids. Recent development and applications. *Laser Phys.* 2009;19:1330–40.
- Santos R, Miranda LCM. Theory of the photothermal radiometry with solids. *J Appl Phys.* 1981;52:4194–8.
- Delenclos S, Dadarlat D, Houriez N, Longuemart S, Kolinsky C, Hadj Sahraoui A. On the accurate determination of thermal diffusivity of liquids by using the photopyroelectric thickness scanning method. *Rev Sci Instrum.* 2007;78:024902.
- Dadarlat D, Neamtu C, Pop R, Marinelli M, Mercuri F. On the selection of the experimental parameters in a thermal-wave-resonator-cavity (TWRC) configuration. *J Optoelectron Adv Mat.* 2007;9:2847–52.
- Shen J, Mandelis A. Thermal-wave resonator cavity. *Rev Sci Instrum.* 1995;66:4999–5005.
- Balderas-Lopez LA, Mandelis A, Garcia JA. Thermal-wave resonator cavity design and measurements of the thermal diffusivity of liquids. *Rev Sci Instrum.* 2000;71:2933–7.
- Dadarlat D, Neamtu C. High performance photopyroelectric calorimetry of liquids. *Acta Chim Slov.* 2009;56:225–36.
- Dadarlat D, Pop MN, Streza M, Longuemart S, Depriester M, Sahraoui AH, Simon V. Combined FPPE–PTR calorimetry involving TWRC technique II. Experimental: application to thermal effusivity measurements of solids. *Int J Thermophys.* 2011. doi 10.1007/s10765-011-1067-y.

19. Pittois S, Chirtoc M, Glorieux C, Bril W, Van den Thoen J. Direct determination of thermal conductivity of solids and liquids at very low frequencies using the photopyroelectric method. *Anal Sci.* 2001;17:S110–3.
20. Menon PC, Rajesh RN, Glorieux C. High accuracy self-calibrating photopyroelectric device for the absolute determination of thermal conductivity and thermal effusivity of liquids. *Rev Sci Instrum.* 2009;80:054904.
21. Streza M, Dadarlat D, Simon V, Prejmerean C, Silaghi-Dumitrescu L. Thermal diffusivity investigations of some dental materials by using photopyroelectric calorimetry. *J Optoelectron Adv Mat Symposia.* 2009;1:70–3.
22. Dadarlat D, Neamtu C. Detection of molecular associations in liquids by photopyroelectric measurements of thermal effusivity. *Meas Sci Technol.* 2006;17:3250–4.
23. Pop MN, Dadarlat D, Streza M, Tosa V. Photopyroelectric investigation of thermal effusivity of binary liquid mixtures by FPPE–TWRC method. *Acta Chim Slov.* 2011;58:549–54.
24. Dadarlat D, Pop MN. New FPPE–TWRC methodology for measuring the thermal parameters of thin solids. *Meas Sci Technol.* 2010;21:105701–5.
25. Bailey RA. Materials properties database (JAHM software). 1999.
26. Dadarlat D, Pop MN. Self-consistent calorimetry of Liquids. *Int J Therm Sci.* 2011. Submitted.
27. Huang L, Liu LS. Simultaneous determination of thermal conductivity and thermal diffusivity of food and agricultural materials using a transient plane-source method. *J Food Eng.* 2009;95:179–85.
28. Incropera FP, DeWitt DP. *Fundamentals of Heat and Mass Transfer.* 4th ed. New York: John Wiley & Sons; 1996.
29. Marin E. Thermal wave physics: principles and applications to the characterization of liquids. *Rev Ciencias Exatas Naturais.* 2004;6:145–69.
30. Touloukian YS, editor. *Thermophysical properties of matter. The thermophysical properties data center data series.* New York: IFI Plenum Press; 1970.
31. Touloukian YS, editor. *Thermophysical Properties of High Temperatures Solid Materials.* New York: MacMillan; 1967.
32. Perry JH. *Chemical Engineering Handbook.* New York: McGraw-Hill; 1963.
33. Pop MN, Dadarlat D. Photopyroelectric measurement of thermal effusivity of volatile liquids. Thermal wave resonator cavity method. *J Optoelectron Adv Mat.* 2011. Submitted.